Making Isolated Renewable Energy Systems More Reliable

Luiz A. de S. Ribeiro†, Osvaldo R. Saavedra†, Shigeaki. L. Lima†, José G. de Matos† and Guilherme Bonan‡

†Electrical Energy Institute, Federal University of Maranhão - São Luís - MA – Brazil

‡R&D Department, CP Eletrônica S.A – Porto Alegre – RS - Brazil

Abstract

A hybrid renewable energy system (HRES) uses several kinds of sources, including wind and solar, to make better use of the natural resources in standalone applications. A common application of HRES is in remote communities, where interconnected electrical grid is unreachable due to economics and physical reasons. Due to the long distance and difficult access to these isolated areas, electrical generation systems used in these applications must be reliable. And the reliability of the system, especially the inverter used to regulate the AC voltage, is one of the main problems associated to these systems, and it is responsible for the lack of confidence in renewable systems at several locations in Brazil. This paper shows the results of using renewable hybrid systems specially designed for isolated areas, focusing attention on reliability, efficiency and expansion flexibility. It presents the system description, mode of operation, inverter design, and experimental results measured in a pilot plant located in Lençóis Island, a small isolated community in the north region of Brazil.

1. INTRODUCTION

The supply of electricity to isolated communities in Brazil and other developing countries, in general, is still done in a precarious way, using diesel generators, which operate for 3 to 4 hours a day [1], [2]. This has happened mostly due to the high cost associated with the expansion of the conventional power grid to these communities. In some cases, technical and environmental constraints also have been factors that have prevented the full electrical service in these communities, especially those located on oceanic islands.

For societies to have or attempt to maintain a sustainable development it is necessary a lot of effort in the discovery and use of renewable energy sources as well as in the increase of the efficiency in the processing of use these energy sources. In this aspect, the electric power generation based on solar photovoltaic and wind turbines technologies has been effective in distributed generation systems and also in standalone systems for supplying isolated communities [3], [4]. In standalone systems, those solutions have been shown appropriate for areas of difficult access, dispersed, with environmental restrictions or with a population formed by low-income people, even when these adverse characteristics represent a difficulty for the sustainability of the designed generation system. Technical and operational troubles, and supply interruptions are difficult to be solved due to the non availability of technical assistance. The delay of remote assistance leads to long periods of lack of electrical service, causing loss of credibility in this kind of system [5], [6]. Thus, to overcome these difficulties, isolated systems must be projected taking into account reliability, minimizing the dependence of maintenance and human intervention, mainly because it is expensive and quite often not available.

2. CRITICAL ISSUES TO FEASIBILITY

The factors that most influence the reliability of standalone systems based on renewable energy are the following [5] - [8]:

1. *Protection coordination:* inadequate coordination leads to increased number of customers without electric service due to faults;
2. *Distribution network in marine environment*: distribution network exposed to aggressive marine environment are more vulnerable to mechanical failures and fatigue, phase- ground faults and hot spots in connections;
3. *Intermittent nature of renewable resources*: solar and wind energies have an intermittent nature, contrasting with the need to provide continuous and reliable energy;
4. *Voltage regulation*: the voltage of power distribution systems generated from intermittent sources must fulfill the power quality standards of conventional distribution systems ;
5. *Short circuits and faults in general*: requires adequate protections;
6. *Power inverter*: the dependence of unique inverter is critical for feasibility;
7. *Maintenance*: distance, natural obstacles and population with poor economic conditions make difficult the maintenance of isolated systems.

These critical issues must be addressed in order to make reliable the operation of isolated renewable energy based systems. A practical example is the system installed on the Island of Lençóis in the northeast of Brazil. This autonomous system was projected to provide electrical power 24 hours a day for a community formed by approximately 390 inhabitants distributed in 90 homes. At the end of 10 years of operation, the full power consumption of the island was estimated to be approximately 6,800 kWh a month. This estimation takes into account the residential, small businesses, public agencies (school and health post) consumptions, and the consumption of a small ice factory with an average of 720 kg / day.

Figure 1 shows a panoramic view of the Island. At right side, wind micro-turbines are observed.

Figure 1. View of island of Lençóis, Maranhão Brazil.

3. MIXING RENEWABLE ENERGY SOURCES

Solar and wind energies are sources frequently available in most of isolated applications. However, they are intermittent in nature, contributing to energy supply with low reliability. To reduce this effect and to improve reliability, a practical solution is to mix these sources, obtaining the so called hybrid systems. Unfortunately, some difficulties still remain: the quality of energy must meet the standards set by regulatory agencies; what to do when all the primitive sources are not available? A well designed renewable hybrid generation system must meet some basic requirements in order to have power quality and its autonomy should be such that it achieves the community expectations. The simplified block diagram of the proposed system is presented in Fig. 2. It is formed by a solar sub-system, a wind sub-system, a battery bank, a back-up diesel generator, an inverter system, and a sub-system of control and management based on a programmable logical controller (PLC).

The solar sub-system is composed of 9 PV' strings in parallel, each one formed by 18 photovoltaic modules in series. The strings were installed on the roof of the powerhouse as illustrated in Fig. 3. Each string has a controller to provide the correct charging of the battery bank. The total maximum power of this sub-system is approximately 21 kWp.

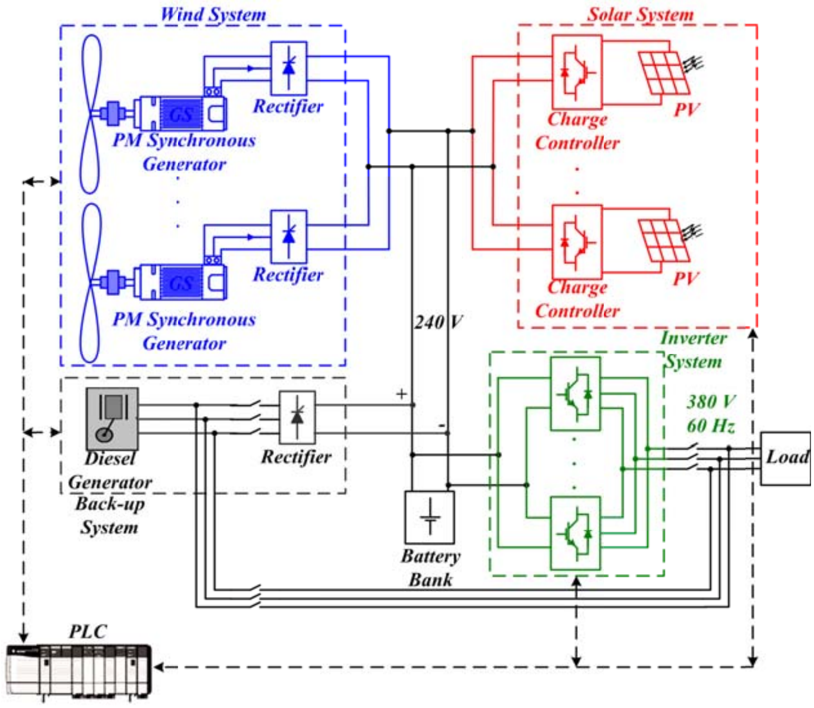

Figure 2. Block diagram of the hybrid power system.

Figure 3. The solar sub-system.

The electrical specifications of the solar modules that were used are shown in Table I. Its electrical characteristics (current versus voltage as a function of temperature and solar irradiation) are shown in Fig. 4.

TABLE I

Electrical Specifications of the solar module

Maximum Power	130 W
Tolerance	+10% / -5%
Maximum Power Voltage	17.6 V
Maximum Power Current	7.39 A
Open Circuit Voltage	21.9 V
Short Circuit Current	8.02 A
Rated temperature for cell operation	47º C
Current temperature coefficient	[3.18 x 10^{-3}] A/Cº
Voltage temperature coefficient	[-8.21 x 10^{-2}] V/Cº

Note: These values are valid under standard tests conditions with irradiation of 1 kW/m^2, Spectrum 1.5 Air Mass and cell temperature equal to 25ºC.

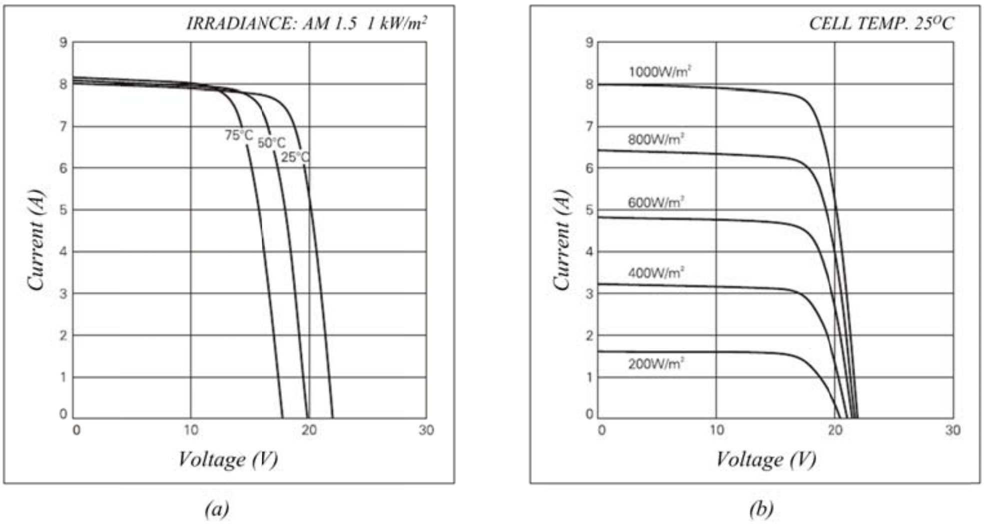

Figure 4. Solar module characteristics of current versus voltage: a) as function of the temperature and b) as function of the solar irradiation

The wind sub-system is formed by three small wind turbines, each one with 3 blades upwind, BCW EXCEL-R/240 model (battery charging version), manufactured by Bergey WindPower [9]. These turbines were installed near the sea, on towers with 30 m high, as shown in Fig. 5. The wind generators are three-phase permanent magnet synchronous type, with an exterior rotor drum type with 38 poles. The AC output voltage is rectified to charge the battery bank. Others technical specifications of each turbine, got from the owner's manual, are presented in Table II. The turbine power curve is shown in Fig. 6 for a sea level site, with air density of 1.225 kg/m^3, 10% of turbulence factor, and 30 m high tower [9].

TABLE II

Specifications of the wind turbines

Start up wind speed	3.1 m/s
Cut-in wind speed	3.5 – 4.5 m/s
Rated wind speed	12.4 m/s
Furling wind speed	15.7 m/s
Maximum design wind speed	54 m/s
Rotor diameter	7 m
Rotor speed	0 - 350 RPM
Rated power with battery charger	7 - 8.5 kW
Output rated voltage	240 VCC

Figure 5. The wind sub-system (tower height: 30 m)

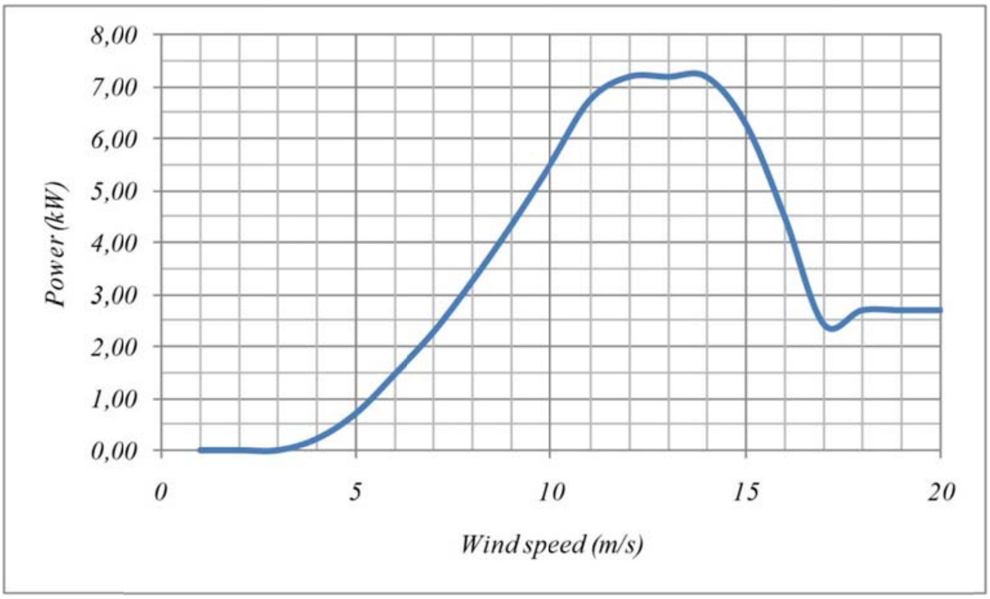

Figure 6. Wind Turbine power curve

The solar and wind sub-systems work in parallel to charge a bank composed of 120 batteries, arranged in 6 parallel strings, each formed by 20 batteries of 150 Ah in series. The nominal voltage of the bank is 240 VDC. The batteries technical specifications, according to the manufacturer data, are summarized in Table III. The system control is configured for a maximum depth of discharge (DOD) of battery bank equal to 30%. With this DOD it is expected that the battery bank can supply the load continuously for 8 hours in case of lack of sun and or wind.

TABLE III

Specifications of the batteries

Rated capacity at 25 °C and 20 hours (C5)	150 Ah
Rated voltage at 25 °C	12 V
Float voltage at 25 °C	13.22 – 13.80 V
Equalization voltage at 25 °C	14.40 – 14.89 V
Indicative voltage of full discharge	10.5 V
Round trip efficiency	≈ 85%
Temperature compensation coefficient	-0.030 V for each 1°C above 25 °C
	+0.030 V for each 1°C below 25 °C

There is also a 53 kVA diesel generator as a backup unit to be used eventually during the lack of the primary energy sources or when the renewable power generation sub-systems are on maintenance.

The DC bus is the input of the inverter sub-system. It is formed by two three-phase inverters, each one with rated power of 20 kVA, configured to work in parallel, sharing equally the load. It is important to notice that there isn't any communication interface between these units or data exchange.

The automatic management of the system is done by a programmable logic controller (PLC), which is responsible by the coordination of the parallel operation of all sources, with special attention to the system efficiency.

The generation system is installed in the Northeast of Brazil, coordinates 1°18'55.81''S and 44°52'41.40''O. The solar potential for electrical generation in this site is summarized in Table IV. These data were obtained from the Brazilian solarimetric map, available in [10]. The installed power of the solar sub-system is 21.06 kW. By considering the functional characteristics of the charger controller and the conversion system efficiency, the net maximum power of the solar sub-system is around 85% of the gross installed power, e.g., 17.69 kW. Multiplying this value by the monthly radiation in kWh/m^2/day and by the number of days in a particular month, it is found an estimate of the monthly generated energy, as shown in last line of Table IV.

TABLE IV

Local solar potential

Month	Jan.	Feb.	Mar.	Apr.	Mar.	June	July	Aug.	Sept.	Oct.	Nov.	Dec.	Year
Radiation in (kWh/m^2)/day	4.06	4.56	3.94	4.03	4.39	4.61	4.97	5.61	5.58	5.69	5.72	5.00	4.85
Days in the month	31	28	31	30	31	30	31	31	30	31	30	31	-
Estimate of the generated energy in kWh/month	2227	2259	2161	2139	2408	2447	2726	3077	2962	3121	3036	2742	31303

The wind potential for electrical energy generation of the area under investigation is summarized in Table V. These data were obtained from the Atlas of the Brazilian Wind Potential, available in [11]. The estimated values for the mean power and the mean generated energy presented in Table V were calculated using the Weibull probability density and the turbines power curve, using the values of the mean wind speed and the Weibull K factor shown in the first two lines of this table [9], [12].

TABLE V

Local wind potential

Month	Jan.	Feb.	Mar.	Apr.	May	June	July	Aug.	Sept.	Oct.	Nov.	Dec.	Year
Mean Wind Speed in m/s	6.25	6.25	5.07	5.07	5.07	7.44	7.44	7.44	8.99	8.99	8.99	6.25	6.94
Weibull K Factor	2.30	2.30	1.97	1.97	1.97	2.66	2.66	2.66	3.60	3.60	3.60	2.30	2.63
Daily Mean Power in kW for 1 turbine	1.97	1.97	1.12	1.12	1.12	2.60	2.60	2.60	3.86	3.86	3.86	1.97	2.39
Daily Mean Gen. Energy in kWh/day with 1 turbine	47.40	47.40	26.90	26.90	26.90	62.30	62.30	62.30	92.70	92.70	92.70	47.40	57.33
Monthly Mean Gen. Energy in kWh/month for 1 turbine	1,469	1,327	834	807	834	1,869	1,931	1,931	2,781	2,874	2,781	1,469	20,908
Monthly Mean Gen. Energy in kWh/month for 3 turbines	4,408	3,982	2,502	2,421	2,502	5,607	5,794	5,794	8,343	8,621	8,343	4,408	62,724

Table VI shows the energy balance between the expected power generation and the expected energy consumption. The residential consumption was estimated considering the expected use of appliances, lighting, etc., by local residents. The productive consumption is related to the installation of a small ice factory to meet the needs of local fishermen. It is also included in the total energy consumption the energy used in public lighting. As can be seen only in March, April, and May it is expected a deficit in the generation from the renewable sources. In these months part of the energy supply is expected to be from the diesel generator. The expected excess of energy in the other months must be discharged.

TABLE VI

Energy balance between estimated generation and estimated consumption

Generated Energy in (kWh)	**Jan.**	**Feb.**	**Mar.**	**Apr.**	**May**	**June**	**July**	**Aug.**	**Sept.**	**Oct.**	**Nov.**	**Dec.**	**Year**
Month	**1**	**2**	**3**	**4**	**5**	**6**	**7**	**8**	**9**	**10**	**11**	**12**	**-**
PV Solar	2,227	2,259	2,161	2,139	2,408	2,447	2,726	3,077	2,962	3,121	3,036	2,742	31,303
Wind	4,408	3,982	2,502	2,421	2,502	5,607	5,794	5,794	8,343	8,621	8,343	4,408	62,724
Total Generation	6,635	6,240	4,663	4,560	4,909	8,054	8,520	8,871	11,305	11,742	11,379	7,150	94,027
Residencial Consumption	4,134	4,139	4,144	4,150	4,155	4,160	4,165	4,170	4,175	4,181	4,186	4,191	49,950
Productive Consumption	1,912	1,912	1,912	1,912	1,912	1,912	1,912	1,912	1,912	1,912	1,912	1,912	22,939
Total Consumption	6,046	6,051	6,056	6,061	6,066	6,071	6,077	6,082	6,087	6,092	6,097	6,103	72,889
(Generation - Consumption)	589	190	**-1,393**	**-1,501**	**-1,157**	1,982	2,443	2,789	5,218	5,650	5,282	1,048	21,138

Table VII shows measurements for solar generation sub-system during the months of March to July of 2010. As can be seen the maximum power generation are of the same order of magnitude as the net installed power of the solar panel, which is 17.67 kW (≈ 0.84 x 21 kW). It is also possible to see that the values measured for the Mean Generated Energy in each month have similar magnitude if they are compared with the estimated values shown in Table IV.

TABLE VII

Measures of power generation with the solar panel on first semester of 2010

Month	Mar.	Apr.	May	June	July
Maximum power generated in kW	16.66	16.98	15.88	16.40	17.08
Daily Mean Power in kW	3.32	2.95	3.29	3.57	3.70
Mean Generated Energy in kWh	2,369.3	2,032.8	2,414.2	2,459.8	2,637.2

Table VIII shows power and energy supplied by just one turbine of the wind generation sub-system from March to July of 2010. The daily average power and average generated energy are relatively smaller than the respective values that were estimated for these variables in Table V. The main reason of this discrepancy was the abnormal wind pattern observed in this specific period as compared to previous years. Another reason for this discrepancy is related to the fact that in the estimation of power generated by one turbine, it was considered as if it was working alone. In the Lençóis Island Generation System, on other hand, the turbines work in parallel with the PV sub-system to charge the same battery bank. So, it is possible that in a particular time more energy is possible to be generated than what is possible to be stored in battery bank. In such conditions, the wind turbine sub-system or the PV sub-system or both generates less energy than what they are capable to generate. So, the value of daily mean power shoed in Table VIII can be smaller than what was estimated and shown in Table VI, without representing error in the estimate of generation capacity of wind turbines.

TABLE VIII

Measures of power generation with the wind power sub-system on first semester of 2010

Month	Mar.	Apr.	May	June	July
Daily Mean Power in kW with 1 turbine	1.35	0.86	0.89	0.90	0.80
Mean Generated Energy by 1 turbine in kWh/day	29.71	18.77	19.39	19.89	17.78

The values of the residential energy consumption during the period from March to July 2010 are presented in Table IX. Fortunately, these values are relatively smaller than the respective estimated values shown in Table VI. This is good for the system, because it is an indication that the system still has the capacity to supply an expansion of consumption in coming years. The reduced consumption compared to the estimated one is mainly due to an educational program related to the efficient use of electricity by the community as well as due to the fact that the community needs to pay for energy consumed.

TABLE IX

Measures of residential energy consumption from March to July of 2011

Month	Mar.	Apr.	May	June	July
Residential Energy Consumption in the first semester of 2011 in kWh	2,908	3,283	3,221	3,436	3,480

4. PARALLEL-CONNECTED INVERTERS

In the project of the inverters, the goal was to develop a system that, besides highly reliable, it also had capacity for expansion as the loads increase without the need of alterations in the equipments already installed. To considerably increase the reliability and robustness of the system, it was adopted parallel operation of the inverters without communication among the units. The MTBF of inverters connected in parallel, in the $N+1$ or $N+2$ configurations, is greater than that of individual equipment, which demonstrates the reliability provided by this type of operation [13], [14]. For the $N+1$ configuration one inverter (N) is able to supply energy to the load. The other inverter ($+1$) is redundant. However, this reliability is only obtained through a system without communication, with units totally autonomous.

Among the several forms used to connect voltage source inverters in parallel, it is possible to classify them in two groups: 1) the systems without communication and 2) the systems with communication. Parallelism with communication, as for instance in master-slave systems, uses an external cable for synchronization of the references and sharing of loads. In the case of a failure in that communication, the whole system can fail, unless another unit assumes the control. Seeking to avoid that type of problem, it was developed a system that works in parallel without any communication among the units. One of the methods more commonly implemented is known as Drooping Method [15] - [18].

5. SYSTEM MODELING

The hardware design was based on a 20kVA, three-phase IGBT inverter. The output 60 Hz voltage was regulated based on a space vector pulse width modulation (SVPWM) with a 4 kHz switching frequency. An output low pass filter was used in each phase to eliminate the high frequency harmonic content due to the inverter switch action. Furthermore, a transformer was used to provide galvanic isolation and change the output voltage level. As a final component there is output impedance used to share equally the load between the units. Besides voltage transformation, this isolation transformer was also used to protect the load and the equipments connected in parallel against fail or isolation loss, improving the reliability and robustness of the overall system. The block diagram of the inverter system is presented in Fig. 7. The control system was designed taking into account each of the blocks shown in this figure. This figure shows two inverters connected in parallel to emphasize the *N+1* operation that was adopted. The system controls the output voltage of each individually inverter and the load share between the units. The output voltages are measured using voltage transformers and the measured voltages are converted to digital form using the analog to digital converters input (ADCIN) of the DSP TMS320LF2407. These values are compared to the reference ones, and generate the errors input to the voltage controllers. The voltage controllers generate the inputs to the SVPWM that generate the pulses to the switches of the inverters. The load share between units is based on the control of the frequency of the output voltages using the drooping method [15] - [18].

In Fig. 8 there is a more precise idea of the voltage control algorithm that was implemented. In this figure it is shown the control block diagram of just one inverter. The other inverters working in parallel have the same control topology. Because there are two controllers, one for each voltage component, the diagram was drawn using rotating vectors: two lines in the diagram stands for voltage vector.

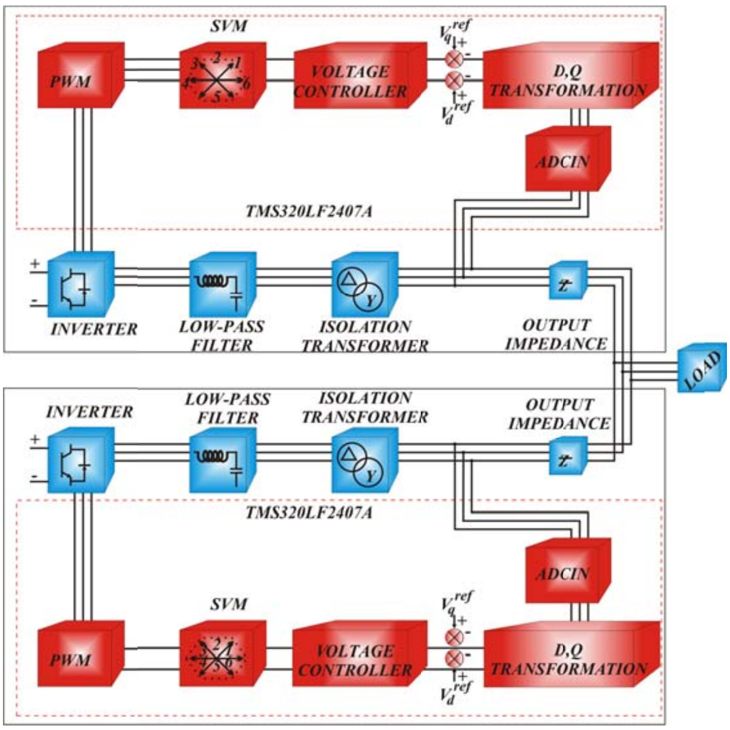

Figure 7. Block diagram of 2 inverters in parallel (N+1).

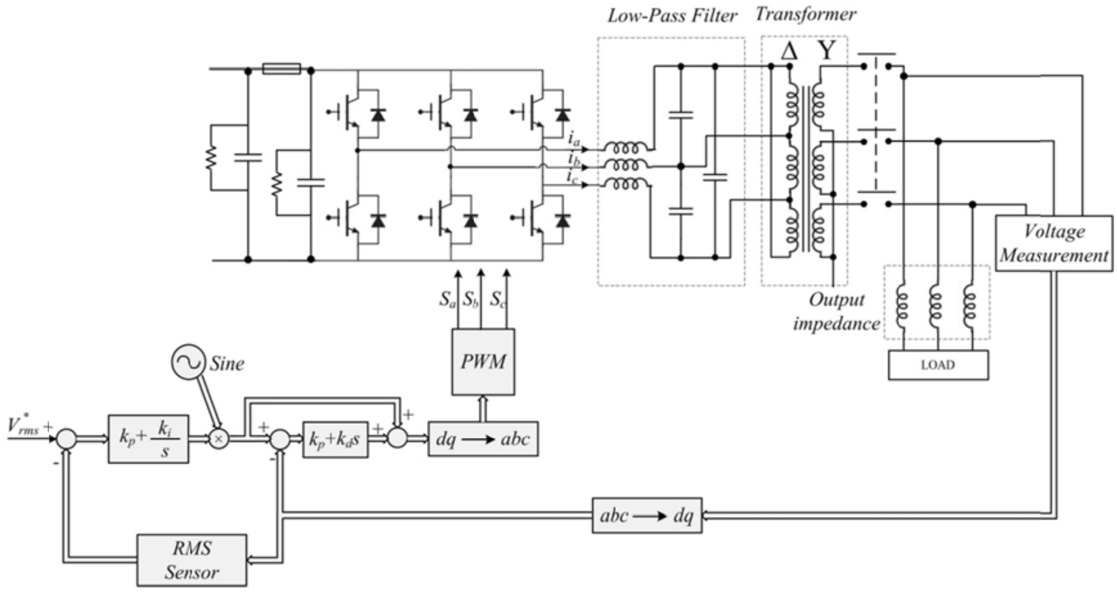

Figure 8. Diagram of the control system

The control of the system is accomplished by two loops: an inner loop responsible for the fastest dynamics, and an outer loop responsible for the slowest dynamics. The inner loop is based on a PD controller that has a widespread use in industry and easy to tune. It is responsible to track the sinusoidal voltage reference. In this inner loop, the PD controller works with sinusoidal signals. To achieve a zero steady state error an outer loop was implemented to control the RMS level of the output voltage through a PI controller. Since the RMS is a dc value to the PI controller, it guarantees zero steady state error. On the other hand, applying a PI controller directly in the inner loop can reduce but will not achieve zero steady state error due the frequency response characteristics of the integral block of the PI controller.

6. PROTECTIONS & COORDINATION

The first thing that was adjusted during the start-up procedure was the general coordination protection against over currents and short circuits. The protection was done by using electromagnetic breakers, type B (standard IEC 898). The nominal current was chosen to be 5 A. This low value is justified based on the installed load in the houses, in general below 500 VA. The type B devices allow the coordination protection against short circuits between the house breakers and the inverters. The actuation of this device for currents above 5 times rated current is in the range of 10 ms. As a result, the breakers open almost instantly for currents above 25 A. This setup was enough to coordinate this protection and the one imposed by the inverters itself that is 32 ms for currents above 1.5 times rated phase current. After this adjust the protection of the system begun operation without failures caused by short circuits.

Another important aspect is the start-up of the inverters after a fault or intentionally turns off for maintenance or any other reason. Because the system and the inverters have limited power the inrush current during the start-up could eventually shut down the inverters. The way the system was designed anytime the inverters have to be turned off for maintenance the diesel generator backup system is turned on. By the time the inverters are turned on the diesel generator is already supplying the load, and there is no inrush current that can cause the inverters shut down when the load is transferred from the diesel generator to the inverters. In case of a fault the following two procedures were tested to mitigate the problems caused by the inrush current:

1) Anytime the system has to be started-up after a fault the following turn on sequence is applied:

- Turn on the diesel generator and supply the load;
- Turn on the first inverter;
- Parallel the other inverters with the first one that was previously turned on;
- Transfer the load to the inverter system;
- Turn off the diesel generator;

2) In the second procedure the load circuits are partitioned. In the case of the proposed system, there are four sectors (north, south, east, and west). The inverters are turned on in the same manner as in the first procedure, and the load is applied sequentially, sector by sector. This second procedure is preferred since it is not necessary to turn on the diesel generator.

The aerial distribution network should be based on insulated cables due to the aggressive marine environment. The public illumination must also be protected against the hazardous environmental conditions. Due to limited energy resources the public illumination is based on compact fluorescent lamps. The solution implemented in the proposed system is presented in Fig. 9.

Figure 9. View of the aerial distribution network

7. PERFORMANCE

Unlike large interconnected systems, in stand-alone systems with light load, power quality varies significantly with the size and type of loads, with major implications in the reliability of operation. Due to government policy for energy efficiency in isolated systems, efficient lamps should be used in homes and public lighting. Typical fluorescent lamps with electronic ballast are used, contributing to degrade the current and voltage waveforms.

In fact, the load current at the Lençóis Island is strongly distorted. But even with this kind of current the controller regulates the inverter voltages with small THD_v. Figs. 10-12 show the voltage, current and instantaneous power of the phases R, S, and T, measured with the systems supplying energy to the entire island.

Through the results presented in Fig. 10-12, it is possible to observe the unbalance of the system due to different loads supplied by the inverters. They were submitted not only to different current waveforms but also to different output current levels (unbalanced operation). Nevertheless, they maintain the output voltage stable and with low distortion level.

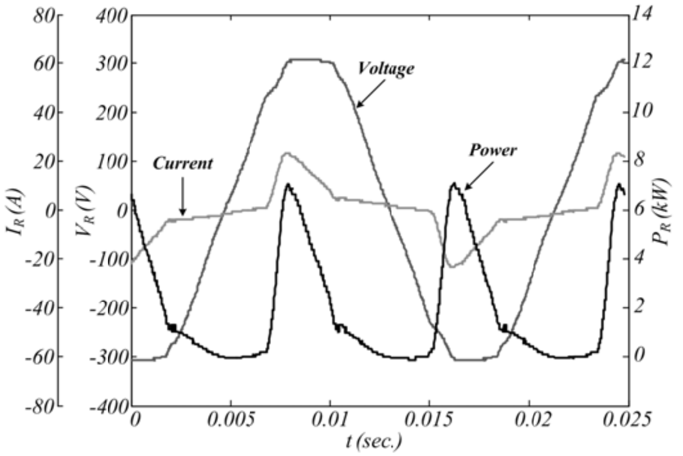

Figure 10. Inverter output voltage, current and instantaneous power of phase R with the system working at the island.

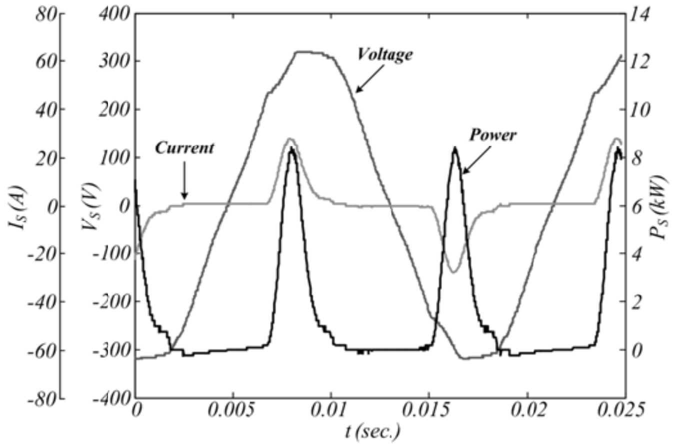

Figure 11. Inverter output voltage, current and instantaneous of phase S with the system working at the island.

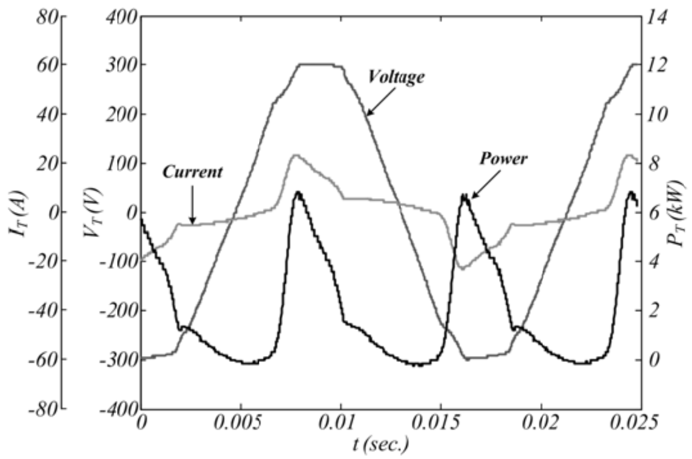

Figure 12. Inverter output voltage, current and instantaneous power of phase T with the system working at the island.

It can be observed that even with a huge current total harmonic distortion (*THD_i*) due to the non linear load of the island (see Fig. 13), the inverter output voltage has a *THD_v* smaller than 5%. This result can be observed in Fig. 14. This *THD_v* level depends on the load conditions.

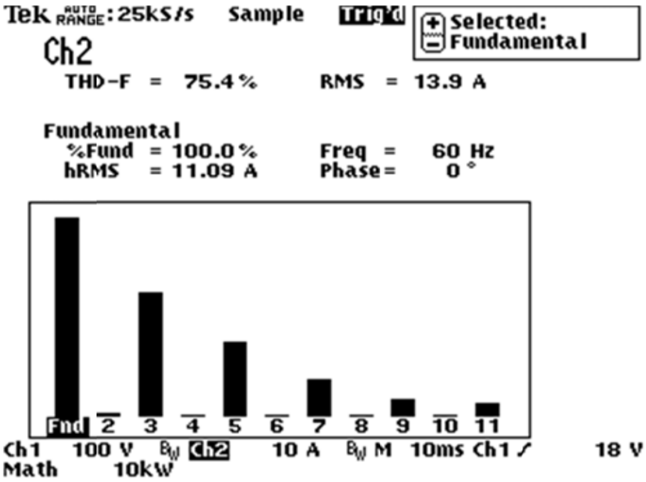

Figure 13. Inverter output current THD with today's island load.

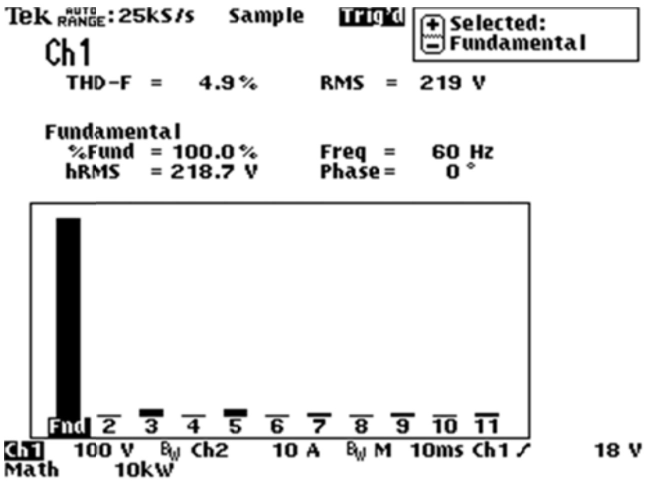

Figure 14. Inverter output voltage THD with today's island load.

8. EFFICIENCY

Another important aspect to be considered is the global efficiency of the equipments. The bigger the efficiency is the better will be the use of the generated energy. Table X shows the efficiency of the inverters measured in the laboratory with the inverters supplying nominal linear load. It must be noted that the efficiency results presented in Table X are different from the results obtained in the island because the load conditions during the tests were different.

TABLE X

Efficiency results

Equipment	Input Power (kW)	Output Power (kW)	Efficiency (%)
Inverter 1	20.5	19.1	93.17
Inverter 2	19.1	17.4	91.09

During the first three years of operation, the load never gets to the values showed in Table X. Instead the peak power was approximately 10 kW. As a result the efficiency measured in the field is smaller than the efficiency measured in the laboratory, especially because the inverters are supplying non-linear, unbalanced loads at Lençóis Island. Figure 15a shows the input and output power measured in a typical day of February, 2010. And Figure 15b shows the efficiency calculated in the same period. The maximum efficiency was approximately 90.5 %, measured at the time when the load is at its maximum.

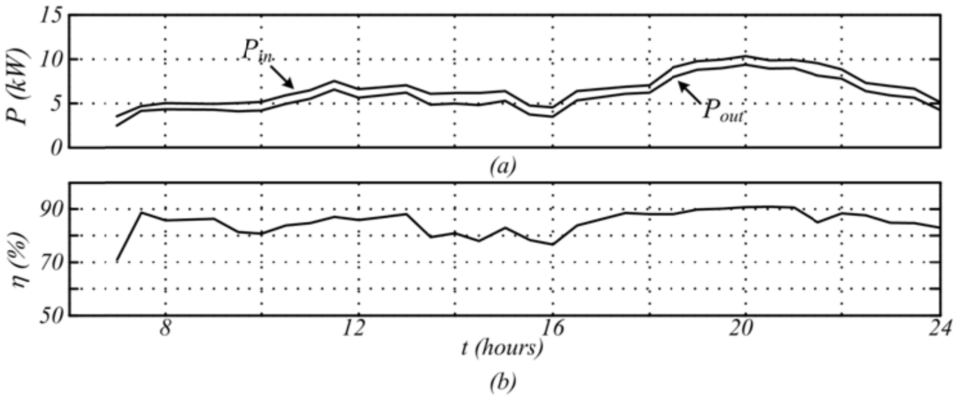

Figure 15. (a) Input and output power of the inverter; (b) efficiency

9. RELIABILITY INDICES

Since July, 20th 2008 the system has been in operation. The first year - 160 days - was considered as a testing period and 2009 – 2011 as steady state operation. There are many indices for measuring reliability. The most common are referred to as SAIFI and SAIDI, defined in IEEE Standard 1366 as system average interruption frequency index and system average interruption duration index, respectively. These indices are equivalent to FEC and DEC, respectively, used in Brazil.

As a reference, a typical distribution company of Sao Paulo, Brazil reported in 2008 SAIFI = 5.87 and SAIDI= 6.85 hours. From July, 20th to December 31st of 2008, the indices obtained from Lençois system were: SAIFI = 3 and SAIDI = 72 hours. In this first year, just 24 hours were provided by diesel generator, representing only 0.609 % of the period (164 days or 3936 hours). Therefore, during 99.390 % of this time the demand was supplied by renewable wind – solar sources.

At the second year (2009), no supply interruptions have been registered, leading to SAIFI =0 and SAIFI =0. These good reliability indices are attributed to the good automation degree of the system and to the small scale distribution network as well, adequately prepared for marine environmental conditions. Table XI summarizes the indices of the system operation over the period 2009 - 2010.

TABLE XI

System operation indices

System Operation				
	SAIFI	SAIDI	Renewable energy operation	Diesel operation
1st year (3936 hours)	3	72	99.390%	0.609 %
2nd year (8760 hours)	0	0	95.43%	4.56%
3rd year (8760 hours)	2	48	92.30%	7.70%

The current and voltage measured in a typical day of December/2009 are showed in Fig. 16, which shows the RMS values of currents and voltages measured in a period of approximately 10 hours. It can be observed that the system is unbalanced and that the currents have high harmonic content since the neutral current is high. Even with this high current harmonic content the variations of the voltages RMS values are within ± 2% of the rated value (220 V).

The total harmonic distortions of the currents (THD_i) and voltage (THD_v) measured in the same day of Fig. 16 are presented in Fig. 17. It can be shown the high THD_i (Fig. 17a) caused by the non-linear loads (fluorescent lamps, TVs, and refrigerators). This distortion and the load unbalance cause a $THD_v > 5\%$ (Fig. 17b) during some hours.

To bring the THD_v to levels within the IEEE recommended practices ($THD_v < 5\%$) it was tested to reduce the amount of unbalance to levels below 50% among the phases. Then part of the load was relocated among the phases. By just doing this simple task the THD_v was improved as can be seen in Fig. 18. These data were measured in February/2010 by the time there was another travel to the island. Even though the data was measured in a different day the results were taken in time intervals were it was observed the worst THD_v.

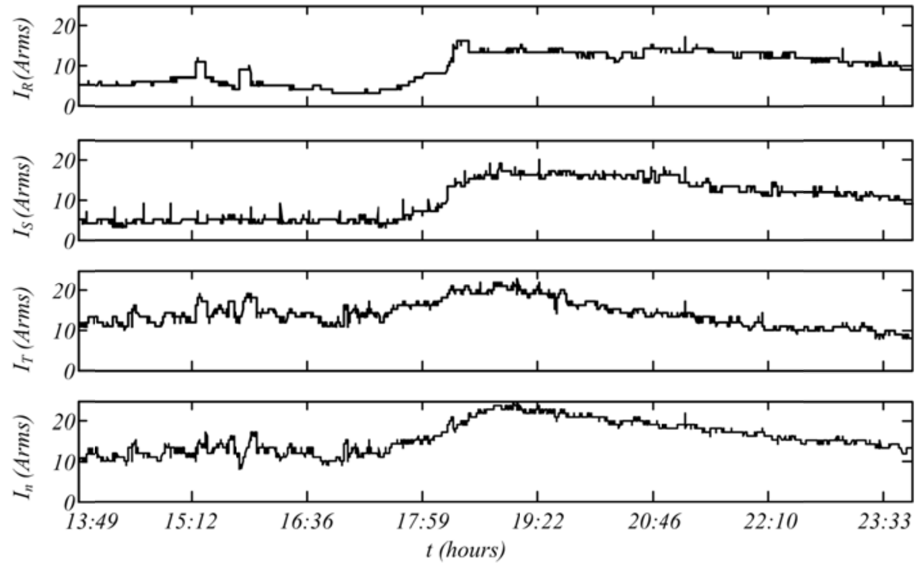

(a)

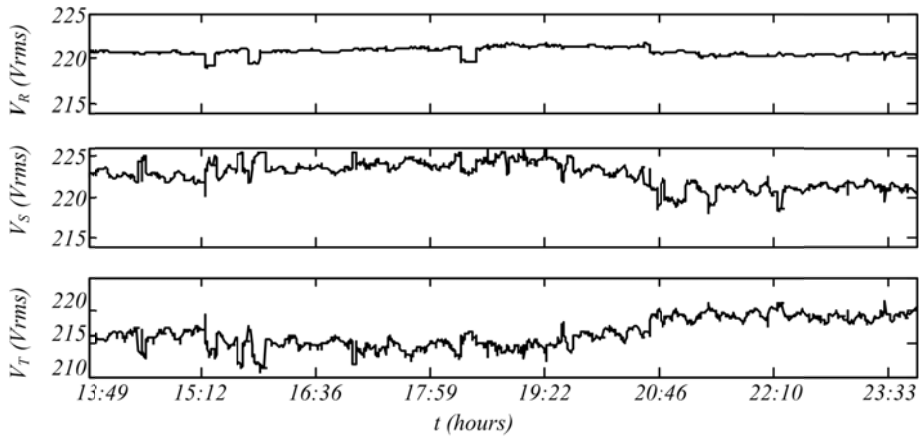

(b)

Figure 16. RMS values of current (a) and voltage (b) measured in December/2009

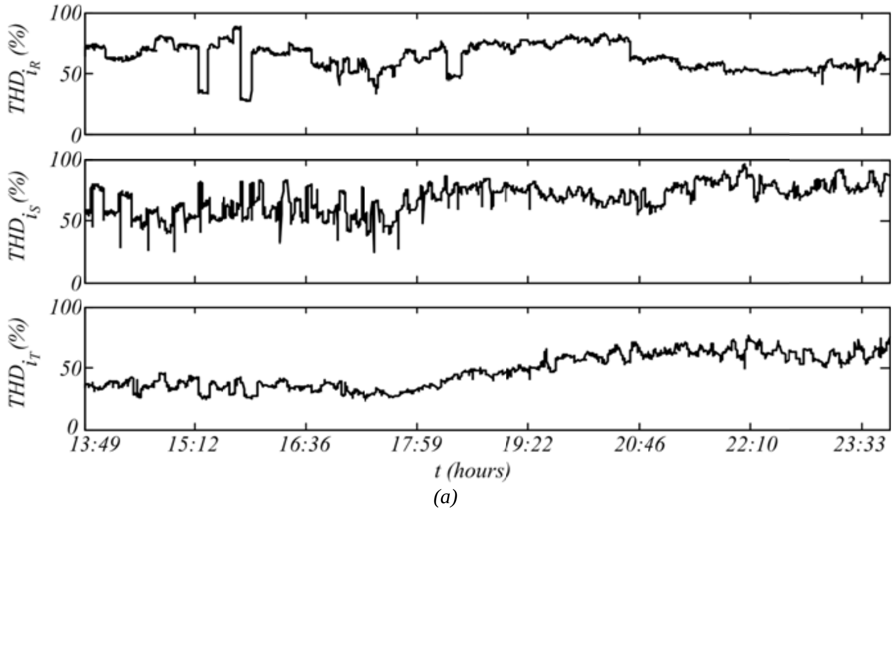

(a)

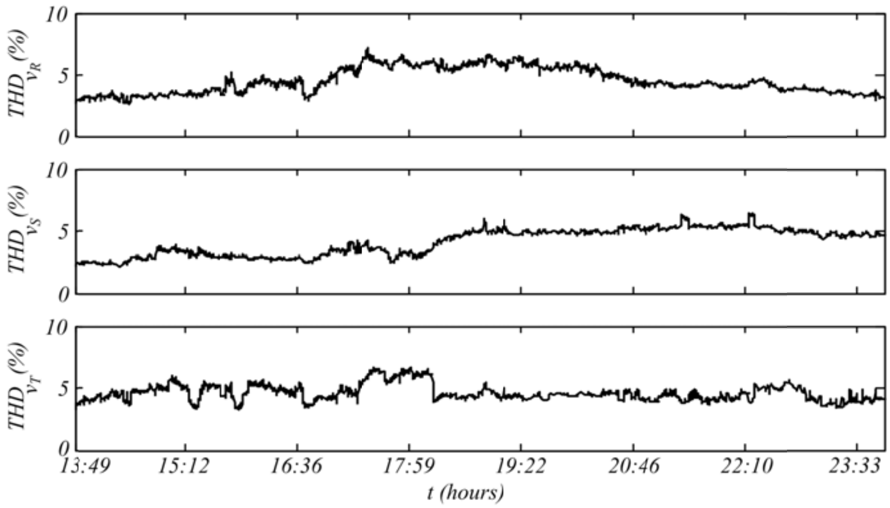

(b)

Figure 17. Total harmonic distortion of currents (a) and voltage (b)

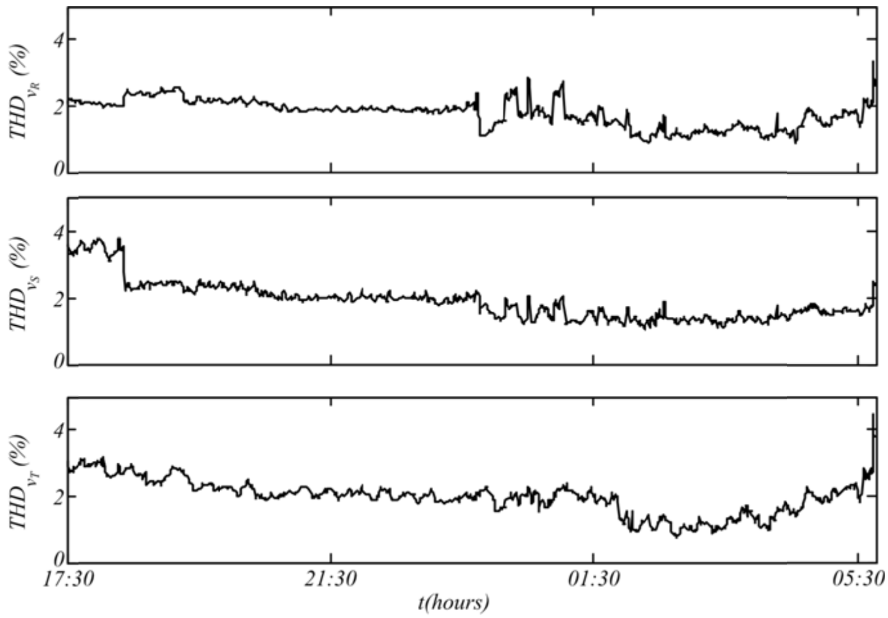

Figure 18. Total voltage harmonic measured after load balance

Figure 19 illustrates the individual contribution of renewable resources and battery bank charge in August, 8, 2009. Negative values indicates that the battery bank in discharging, i.e., it is complementing the load balance. For this day, a slight complementary behavior among solar and wind energies is observed. In general, this behavior cannot be sustained over several months. Typically, hot and sunny days are accompanied by winds.

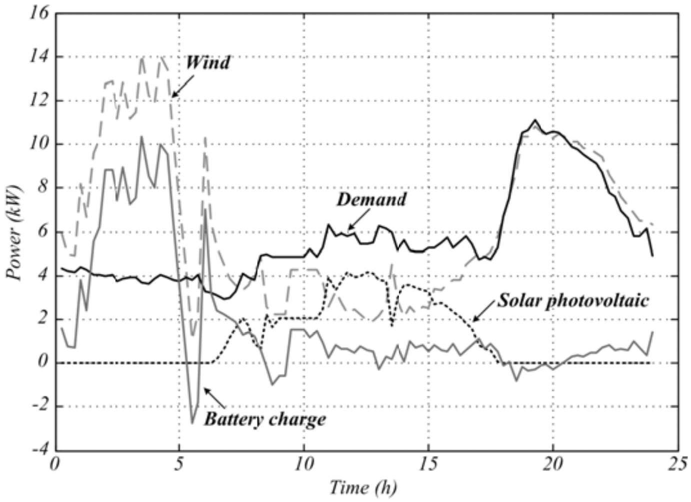

Figure 19. Daily participation of renewable sources and battery bank

10. CONCLUSIONS

Fulfilling a few critical issues it is possible turn reliable renewable hybrid generation systems based on solar photovoltaic and wind energies. These systems definitely help to bring energy to isolated islands and decrease the CO_2 emissions. However, due to the low energy demand and difficult access to isolated areas it is necessary to build a system that is reliable, efficient and presents enough flexibility to load increases. It was shown that these requirements can be fulfill with parallel operation of inverters specially designed for these applications, adequate automation level, practical protection coordination, and using a distribution network adapted to local climate conditions. Experimental results show that the power quality supplied to the consumers is very good. The main feature to be pursued is the reliability of the system, mainly the reliability of the inverters that can be improved by parallel operation.

The practical experience reported here shows the robustness of the system when submitted to load step variations, non linear loads, and the advantages of parallel operation. The system is working in perfect conditions since June 2008 at Lençóis Island, Cururupu, MA, northeast of Brazil.

REFERENCES

[1] L. A. S. Ribeiro, O. R. Saavedra, J. G. Matos, G. Bonan, and A. S. Martins, “Small Renewable Hybrid System for Stand Alone Applications,” *in IEEE Symposium on Power Electronics and Machines in Wind Applications (PEMWA 2009)*, Lincoln, Nebraska, pp. 1 - 7, 2009.

[2] L. A. S. Ribeiro, O. R. Saavedra, J. G. Matos, S. L. Lima and, G. Bonan, and A. S. Martins, "Isolated Micro-Grid With Renewable Hybrid Generation: The case of Lençóis Island," *IEEE Transactions on Sustainable Energy*, vol. 2, no. 1, pp. 1 - 11, January 2010.

[3] L. Flowers, I. Baring-Gould, J. Bianchi, D. Corbus, S. Drouilhet, D. Elliott, V. Gevorgian, A. Jimenez, P. Lilienthal, C. Newcomb, and R. Taylor. "Renewables for Sustainable Village Power," *in American Wind Energy Association's WINDPOWER 2000 Conference*, Palm Springs, California, pp. 1 - 10, November 2000.

[4] E. I. Baring-Gould, C. Newcomb, D. Corbus, and R. Lalidas, R. "Field Performance of Hybrid Power Systems," *in American Wind Energy Association's WINDPOWER 2001 Conference*, Washington, D.C., pp. 1 -10, September 2001.

[5] R. E. Foster, R. C. Orozco, and A. R. P, Rubio, "Lessons Learned from the Xcalak Hybrid System: a Seven Year Retrospective," *in Proc. of 1999 Solar World Conference, International Solar Energy Society*, vol. I, pp. 319-328, Jerusalem, July 1999.

[6] D. Corbus, C. Newcomb, and Z. Yewdall, "San Juanico Hybrid Power System Technical and Institutional Assessment," *in Proc. of World Renewable Energy Congress VIII (WREC VIII)*, pp. 1-5, Denver, Colorado, August 2004.

[7] H. Jiayi, J. Chuanwen, and X. Rong, "A review on distributed energy resources and MicroGrid," *Elsevier Renewable & Sustainable Energy Reviews"*, vol. 12, no. 9, pp. 2472-2483, June 2007.

[8] V. C. Nelson, R. E. Foster, R. N. Clark, and D. Raubenheimer, "Wind Hybrid System Technology Characterization," *NREL – National Renewable Energy Laboratory*, 50 p., 2002.

[9] Bergey Windpower Co. (2011, Maio) [Online]. www.bergey.com.

[10] Cresesb (2011, August) [Online]. http://www.cresesb.cepel.br/sundata/index.php#sundata.

[11] Cresesb (2011, August) [Online]. http://www.cresesb.cepel.br/atlas_eolico/index.php.

[12] J. F. Manwell, J. G. Mcgowan, and A. L. Rogers, *Wind Energy Explained: theory, design, and application*, John Wiley & Sons, Ltd, 2nd Edition, Chichester, England, 2009.

[13] A. P. Wood, "Reliability-Metric Varieties and Their Relationships," in Proc. of the Reliability and Maintainability Symposium, pp. 110 – 115, 2001.

[14] E. E. Lewis, Introduction to Reliability Engineering, John Wiley & Sons Inc., 1987.

[15] J. M. Guerrero, L. Garcia de Vicuña, J. Matas, M. Castilla, and J. Miret, "A Wireless Controller to Enhance Dynamic Performance of Parallel Inverters in Distributed Generation Systems," IEEE Trans. on Power Electronics, vol. 19, no. 5, pp. 1205 –1213, Sep. 2004.

[16] Z. Chen and Y. Hu, "Control of Power Electronic Converters for Distributed Generation Units," in Proc. of IECON 2005 Conf., pp. 1317-1322, Nov. 2005.

[17] Z. Chen, Y. Hu, and F. Blaabjerg, "Control of Distributed Power Systems," in Proc. IPEMC 2006, vol. 3, pp. 1-6.

[18] K. De Brabandere, B. Bolsens, J. Van Keybus, A. Woyte, j. Driesen and, R. Belmans, “A Voltage and Frequency Droop Control Method for Parallel Inverters,” IEEE Trans. on Power Electronics, vol. 22, no. 4, pp. 1107–1115, July 2007.